Chapter 4

Transportation of particulate suspension in a Newtonian fluid by dilating peristaltic waves in a tube of uniform cross-section: Application to flows in normal oesophagus

4.1 Introduction

Solid particles, in practice, are dragged by fluids they are suspended in. There are several flows in nature similar to it. A few of them are physiological flows such as swallowing, blood flows, transportation in intestines, flows of infected urine in the ureters etc. In industries and nuclear plants, we use similar mechanism for

transportation. In food industries as well, this technique of transportation is of immense help.

Peristaltic transport in a channel of a fluid with suspended solid particles was modelled by Hung and Brown (1976) for various geometric and dynamic effects. Drew (1979; 1983) presented a two-phase model for a mixture of dispersed small particles in a fluid as the working medium. Srivastava and Srivastava (1989) used Drew's model (1979) to model a two-phase particle-fluid mixture flowing peristaltically in a channel. They obtained closed form solution using perturbation technique. A model for diseased urine flowing peristaltically through the ureters was further investigated by Misra and Pandey (1994). Jimenez-Lozano *et al*. (2011) also presented a peristalticmodel for uretersthat deals with the flow mechanics of a particle-fluid mixture. Another model for peristaltic flow in uniform and non-uniform annuli with particle-fluid mixture was reported by Mekheimer and Abdelmaboud (2008). A series of recent publications in peristalsis shows how popular the Drew's model is (Bhatti and Zeeshan, 2016a; Bhatti *et al.*, 2016; Bhatti *et al.*, 2017a; Zeeshan *et al.*, 2017; Bhatti *et al.*, 2017b; Bhatti *et al.*, 2018) and rheological flow of blood (Bhatti *et al.*, 2016b; Zeeshan *et al.*, 2018).

Food gulped through the mouth swallows through the pharynx into the oesophagus during deglutition. The journey culminates when the bolus enters into the stomach by peristaltic contractions of the wall. Many of the masticated food are as particulate suspension dragged by an aqueous solution. Pasta products in sauces, yogurts with fruits, fruit preserves with seeds, vegetable soups, fruit in syrup, sugarcane juice with kiwifruit, some other homemade food items (Martinez-Padilla, 2009) are a few instances. Generally, these food items possess non-Newtonian nature but once the volume fraction of suspended particles

is small, they behave almost as a Newtonian fluid. Suspensions are defined as heterogeneous or homogeneous substance with rigid or deformable particles suspended therein. Swallowing of food suspensions is a two-phase flow model

Achalasia causes inadequate lower sphincter relaxation of oesophagus. This hinders oesophageal clearance. Patients may be treated with drugs or by operation (Spechler and Castell, 2001). This analysis aims at finding an alternative complementary way.

A particulate matter cannot move itself but may be dragged by the fluid suspending it. Since the two phases will have different velocities, the analysis may probe which one leads and which one lags behind and some more queries.

Pandey and Singh (2018) attempted to model oesophageal swallowing of particulate suspension in a Newtonian fluid to examine the impact of the presence and concentration of suspended particles in the food. They assumed the peristaltic model of dilating wave amplitude discovered by Pandey *et al*. (2017) which creates higher pressure in the distal oesophagus. They used a regular perturbation technique, for dimensionless quantities, in terms of the wave number in which the wave number is small but not zero. Flow variables were presented in power series of the wave number to obtain closed form solutions up to the first order to put aside evaluation of involved terms of the higher order equations. We tried to evaluate the second order terms to make the solutions more accurate in quantitative terms, easy to accept and also to observe if absence of the second order terms left the solutions crude.

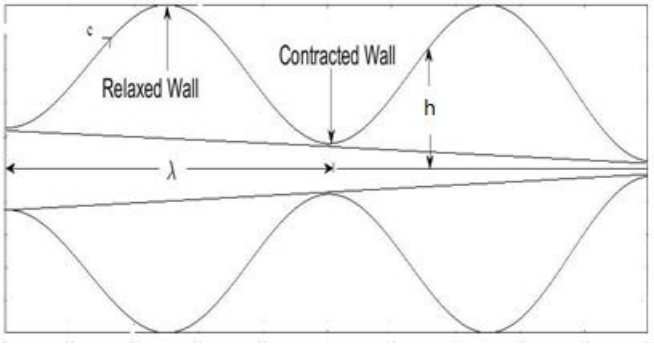

Figure 4.1: The schematic diagram of wall positions of oesophagus when a peristaltic wave of slightly dilating amplitude propagates along it with velocity c.

4.2 Mathematical Formulation

We consider the following wave motion formulated by Pandey *et al*. (2017) to propagate along the walls of the oesophagus considered as a circular cylindrical tube:

$$\tilde{h}(\tilde{x},\tilde{\omega},\tilde{t}) = a - \tilde{\phi}\, e^{\tilde{\omega}\tilde{x}} \cos^2 \frac{\pi}{\lambda}(\tilde{x} - c\tilde{t}), \tag{4.1}$$

where $\tilde{h}$, $\tilde{x}$, $\tilde{t}$, a, $\tilde{\phi}$, $\tilde{\omega}$, λ and c stand respectively for the radial wall displacement, axial coordinate, time coordinate, tube-radius, wave amplitude, amplitude dilation parameter, wavelength and wave velocity (Figure 4.1).

The following are the governing equations separately for the fluid and the suspended particles formulated in the two–phase model of Drew (1979):

Fluid phase equations:

$$\frac{\partial}{\partial \tilde{x}}[(1-C)\tilde{u}_f] + \frac{1}{\tilde{r}}\frac{\partial}{\partial \tilde{r}}[(1-C)\tilde{r}\tilde{v}_f] = 0, \tag{4.2}$$

$$\rho_f(1-C)\left(\frac{\partial \tilde{v}_f}{\partial \tilde{t}} + \tilde{u}_f\frac{\partial \tilde{v}_f}{\partial \tilde{x}} + \tilde{v}_f\frac{\partial \tilde{v}_f}{\partial \tilde{r}}\right) = -(1-C)\frac{\partial \tilde{p}}{\partial \tilde{r}} + \mu_s(C)(1-C)\left\{\frac{\partial^2 \tilde{v}_f}{\partial \tilde{x}^2} + \frac{\partial}{\partial \tilde{r}}\left(\frac{1}{\tilde{r}}\frac{\partial(\tilde{r}\tilde{v_f})}{\partial \tilde{r}}\right)\right\} + CS(\tilde{v_p} - \tilde{v_f}), \quad (4.3)$$

$$\rho_f(1-C)\left(\frac{\partial \tilde{u}_f}{\partial \tilde{t}} + \tilde{u}_f\frac{\partial \tilde{u}_f}{\partial \tilde{x}} + \tilde{v}_f\frac{\partial \tilde{u}_f}{\partial \tilde{r}}\right) = -(1-C)\frac{\partial \tilde{p}}{\partial \tilde{x}} + \mu_s(C)(1-C)\left\{\frac{\partial^2 \tilde{u}_f}{\partial \tilde{x}^2} + \frac{1}{\tilde{r}}\frac{\partial}{\partial \tilde{r}}\left(\tilde{r}\frac{\partial \tilde{u_f}}{\partial \tilde{r}}\right)\right\} + CS(\tilde{u_p} - \tilde{u_f}), \quad (4.4)$$

Particle phase equations:

$$\frac{\partial}{\partial \tilde{x}}(C\tilde{u}_p) + \frac{1}{\tilde{r}}\frac{\partial}{\partial \tilde{r}}(C\tilde{r}\tilde{v}_p) = 0, \quad (4.5)$$

$$\rho_p C\left(\frac{\partial \tilde{v}_p}{\partial \tilde{t}} + \tilde{u}_p\frac{\partial \tilde{v}_p}{\partial \tilde{x}} + \tilde{v}_p\frac{\partial \tilde{v}_p}{\partial \tilde{r}}\right) = -C\frac{\partial \tilde{p}}{\partial \tilde{r}} + CS(\tilde{v_f} - \tilde{v_p}), \quad (4.6)$$

$$\rho_p C\left(\frac{\partial \tilde{u}_p}{\partial \tilde{t}} + \tilde{u}_p\frac{\partial \tilde{u}_p}{\partial \tilde{x}} + \tilde{v}_p\frac{\partial \tilde{u}_p}{\partial \tilde{r}}\right) = -C\frac{\partial \tilde{p}}{\partial \tilde{x}} + CS(\tilde{u_f} - \tilde{u_p}), \quad (4.7)$$

where $\tilde{u}_f$, $\tilde{v}_f$, $\tilde{u}_p$, $\tilde{v}_p$, ρ_f, ρ_p, C, $\rho_f(1-C)$, $\rho_p C$, $\tilde{p}$, S and $\mu_s(C)$ stand respectively for axial and radial velocities of the fluid phase, axial and radial velocities of the particle phase, the original fluid-density, the original particle-material-density, volume fraction of the particulate matter, fluid phase density, particle phase density, pressure, drag coefficient of interaction for the mutually exerted force by the two phases and the effective particulate viscosity.

For the current problem, we use the Stokes drag coefficient for a small particle at low Reynolds number, $S = 9\mu_0/4{r_p}^2$, and Einstein's formula, $\mu_e = \mu_0\,\mu_r$, where μ_0 is the fluid viscosity, r_p is the particle radius and $\mu_r(C) = 1+5/2C$, (Drew, 1979).

Various parameters are non-dimensionalised as follows:

$$x = \frac{\tilde{x}}{\lambda}, r = \frac{\tilde{r}}{\lambda}, t = \frac{c\tilde{t}}{\lambda}, u_f = \frac{\tilde{u_f}}{c}, v_f = \frac{\tilde{v_f}}{c\delta}, u_p = \frac{\tilde{u_p}}{c}, v_p = \frac{\tilde{v_p}}{c\delta}, \delta = \frac{a}{\lambda},$$
$$h = \frac{\tilde{h}}{a}, \rho = \frac{\rho_p}{\rho_f}, \phi = \frac{\tilde{\phi}}{a}, p = \frac{\tilde{p}a\delta}{\mu_s c}, Re_0 = \frac{ac\rho_f}{\mu_0}, Q = \frac{\tilde{Q}}{\pi a^2 c},$$
$$\omega = \tilde{\omega}\lambda, Re = \delta Re_0, M = \frac{9}{4}\left(\frac{a}{r_p}\right)^2 \quad (4.8)$$

where δ, Re_0, Re and M denote respectively the wave number, the Reynolds number, the modified Reynolds number and the drag parameter.

Using equation (4.8), the governing equations (4.1) -(4.7) reduce to

$$h(x,\omega,t) = 1 - \phi\, e^{\omega x}\cos^2\pi(x-t), \quad (4.9)$$

$$\frac{\partial}{\partial x}[(1-C)u_f] + \frac{1}{r}\frac{\partial}{\partial r}[(1-C)rv_f] = 0, \quad (4.10)$$

$$\delta^3 Re_0(1-C)\left(\frac{\partial v_f}{\partial t} + u_f\frac{\partial v_f}{\partial x} + v_f\frac{\partial v_f}{\partial r}\right) = -\mu_r(1-C)\frac{\partial p}{\partial r} + \mu_r(1-C)\left\{\delta^4\frac{\partial^2 v_f}{\partial x^2} + \delta^2\frac{\partial}{\partial r}\left(\frac{1}{r}\frac{\partial(rv_f)}{\partial r}\right)\right\} + \delta^2 CS(v_p - v_f), \quad (4.11)$$

$$\delta Re_0(1-C)\left(\frac{\partial u_f}{\partial t}+u_f\frac{\partial u_f}{\partial x}+v_f\frac{\partial u_f}{\partial r}\right)=-\mu_r(1-C)\frac{\partial p}{\partial x}+\mu_r(1-C)\left\{\delta^2\frac{\partial^2 u_f}{\partial x^2}+\frac{1}{r}\frac{\partial}{\partial r}\left(r\frac{\partial u_f}{\partial r}\right)\right\}+CM(u_p-u_f), \quad (4.12)$$

$$\frac{\partial}{\partial x}(Cu_p)+\frac{1}{r}\frac{\partial}{\partial r}(Crv_p)=0, \quad (4.13)$$

$$\rho CRe_0\delta^3\left(\frac{\partial v_p}{\partial t}+u_p\frac{\partial v_p}{\partial x}+v_p\frac{\partial v_p}{\partial r}\right)=-C\mu_r\frac{\partial p}{\partial r}+CS\delta^2(v_f-v_p), \quad (4.14)$$

$$\rho CRe_0\delta\left(\frac{\partial u_p}{\partial t}+u_p\frac{\partial u_p}{\partial x}+v_p\frac{\partial u_p}{\partial r}\right)=-C\mu_r\frac{\partial p}{\partial x}+CS(u_f-u_p). \quad (4.15)$$

Non-dimensional boundary conditions for the current problem are as follows:

$$u_f=0 \text{ at } r=h, \frac{\partial u_f}{\partial r}=0 \text{ at } r=0,$$

$$v_f = 0 \text{ at } r = 0, v_f = \frac{\partial h}{\partial t} \text{ at } r = h,$$
$$\frac{\partial u_p}{\partial r} = 0, v_p = 0 \text{ at } r = 0. \tag{4.16}$$

4.3 Perturbation Solution

The regular perturbation expansion in terms of the wave number $\delta(<< 1)$, is used to solve the problem under the assumptions that particle volume fraction C is low and is of the form $C = \delta C^{(1)}$. We assume the solutions for the fluid and particle velocities and the pressure of the form

$$u_f(x,r,t) = {u_f}^{(0)} + \delta {u_f}^{(1)} + \delta^2 {u_f}^{(2)} + ..., \tag{4.17}$$
$$v_f(x,r,t) = {v_f}^{(0)} + \delta {v_f}^{(1)} + \delta^2 {v_f}^{(2)} + ..., \tag{4.18}$$
$$u_p(x,r,t) = {u_p}^{(0)} + \delta {u_p}^{(1)} + \delta^2 {u_p}^{(2)} + ..., \tag{4.19}$$
$$v_p(x,r,t) = {v_p}^{(0)} + \delta {v_p}^{(1)} + \delta^2 {v_p}^{(2)} + ..., \tag{4.20}$$
$$p(x,r,t) = p^{(0)} + \delta p^{(1)} + \delta^2 p^{(2)} + ... \tag{4.21}$$

Using equations (4.17) - (4.21) into the equations (4.10) - (4.15), and comparing the coefficients of like powers of δ, we get a set of equations as:

The zeroth-order system of equations is

$$\frac{\partial}{\partial x}[{u_f}^{(0)}] + \frac{1}{r}\frac{\partial}{\partial r}[r{v_f}^{(0)}] = 0, \tag{4.22}$$

$$\frac{\partial p^{(0)}}{\partial r} = 0, \tag{4.23}$$

$$\frac{\partial p^{(0)}}{\partial x} = \frac{1}{r}\frac{\partial}{\partial r}\left(r\frac{\partial {u_f}^{(0)}}{\partial r}\right), \tag{4.24}$$

Under the boundary conditions:

$${u_f}^{(0)} = 0 \text{ at } r = h, \frac{\partial {u_f}^{(0)}}{\partial r} = 0 \text{ at } r = 0,$$

$${v_f}^{(0)} = 0 \text{ at } r = 0, {v_f}^{(0)} = \frac{\partial h}{\partial t} \text{ at } r = h, \tag{4.25}$$

The first-order system of equations is

$$\frac{\partial}{\partial x}[{u_f}^{(1)}] + \frac{1}{r}\frac{\partial}{\partial r}[r{v_f}^{(1)}] = 0, \tag{4.26}$$

$$\frac{\partial p^{(1)}}{\partial r} + \frac{3}{2}C^{(0)}\frac{\partial p^{(0)}}{\partial r} = 0, \tag{4.27}$$

$$\begin{aligned} Re_0\left(\frac{\partial {u_f}^{(0)}}{\partial t} + {u_f}^{(0)}\frac{\partial {u_f}^{(0)}}{\partial x} + {v_f}^{(0)}\frac{\partial {u_f}^{(0)}}{\partial r}\right) = &-\frac{\partial p^{(1)}}{\partial x} - \frac{3}{2}C^{(1)}\frac{\partial p^{(0)}}{\partial x} \\ &+ \frac{3}{2}\frac{1}{r}\frac{\partial}{\partial r}\left(r\frac{\partial {u_f}^{(0)}}{\partial r}\right) + \frac{1}{r}\frac{\partial}{\partial r}\left(r\frac{\partial {u_f}^{(0)}}{\partial r}\right)\Bigg\} + MC^{(1)}({u_p}^{(0)} - {u_f}^{(0)}), \end{aligned} \tag{4.28}$$

$$C^{(1)}\left(\frac{\partial {u_p}^{(0)}}{\partial x}+\frac{1}{r}\frac{\partial}{\partial r}\left(r\frac{\partial (r{v_p}^{(0)})}{\partial r}\right)\right)=0, \tag{4.29}$$

$$C^{(1)}\frac{\partial p^{(0)}}{\partial r}=0, \tag{4.30}$$

$$C^{(1)}\frac{\partial p^{(0)}}{\partial r}=MC^{(1)}(u_f^{(0)}-u_p^{(0)}), \tag{4.31}$$

Under the boundary conditions:

$$\begin{aligned} &{v_p}^{(0)}=0 \text{ at } r=h, {u_f}^{(1)}=0 \text{ at } r=h, \frac{\partial {u_f}^{(1)}}{\partial r}=0 \text{ at } r=0,\\ &{v_f}^{(1)}=0 \text{ at } r=0, \frac{\partial {u_p}^{(0)}}{\partial r}=0 \text{ at } r=0, \end{aligned} \tag{4.32}$$

The Second-order system of equations is

$$\frac{\partial}{\partial x}[{u_f}^{(2)}]+\frac{1}{r}\frac{\partial}{\partial r}[r{v_f}^{(2)}]=0, \tag{4.33}$$

$$\frac{\partial p^{(2)}}{\partial r}+\frac{3}{2}C^{(1)}\frac{\partial p^{(1)}}{\partial r}-\frac{5}{2}{C^{(1)}}^2\frac{\partial p^{(0)}}{\partial r}=0, \tag{4.34}$$

$$Re_0\Bigg[\Bigg(\frac{\partial {u_f}^{(1)}}{\partial t}+{u_f}^{(1)}\frac{\partial {u_f}^{(0)}}{\partial x}+{u_f}^{(0)}\frac{\partial {u_f}^{(1)}}{\partial x}+{v_f}^{(1)}\frac{\partial {u_f}^{(0)}}{\partial r}+{v_f}^{(0)}\frac{\partial {u_f}^{(1)}}{\partial r}\Bigg)$$
$$-C^{(1)}\Bigg(\frac{\partial {u_f}^{(0)}}{\partial t}+{u_f}^{(0)}\frac{\partial {u_f}^{(0)}}{\partial x}+{v_f}^{(0)}\frac{\partial {u_f}^{(0)}}{\partial r}\Bigg)\Bigg]=$$
$$-\frac{\partial p^{(2)}}{\partial x}-\frac{3}{2}C^{(1)}\frac{\partial p^{(1)}}{\partial x}+\frac{5}{2}{C^{(1)}}^2\frac{\partial p^{(0)}}{\partial x}+\frac{1}{r}\frac{\partial}{\partial x}\Bigg(r\frac{\partial {u_f}^{(2)}}{\partial r}\Bigg)$$
$$-\frac{5}{2}{C^{(1)}}^2\frac{1}{r}\frac{\partial}{\partial r}\Bigg(r\frac{\partial {u_f}^{(0)}}{\partial r}\Bigg)+\frac{3}{2}C^{(1)}\frac{1}{r}\frac{\partial}{\partial r}\Bigg(r\frac{\partial {u_f}^{(1)}}{\partial r}\Bigg)+MC^{(1)}({u_p}^{(1)}-{u_f}^{(1)}), \quad (4.35)$$

$$C^{(1)}\Bigg(\frac{\partial {u_p}^{(1)}}{\partial x}+\frac{1}{r}\frac{\partial (r{v_p}^{(1)})}{\partial r}\Bigg)=0, \quad (4.36)$$

$$C^{(1)}\frac{\partial p^{(1)}}{\partial r}+\frac{5}{2}{C^{(1)}}^2\frac{\partial p^{(0)}}{\partial r}=0, \quad (4.37)$$

$$\rho Re_0 C^{(1)}\Bigg(\frac{\partial {u_p}^{(0)}}{\partial t}+{u_p}^{(0)}\frac{\partial {u_p}^{(0)}}{\partial x}+{v_p}^{(0)}\frac{\partial {u_p}^{(0)}}{\partial r}\Bigg)=-C^{(1)}\frac{\partial p^{(1)}}{\partial x}$$
$$-\frac{5}{2}{C^{(1)}}^2\frac{\partial p^{(0)}}{\partial x}+MC^{(1)}({u_f}^{(1)}-{u_p}^{(1)}). \quad (4.38)$$

under the boundary conditions

$${u_f}^{(2)}=0 \text{ at } r=h, \frac{\partial {u_f}^{(2)}}{\partial r}=0 \text{ at } r=0, {v_f}^{(2)}=0 \text{ at } r=0,$$
$${v_p}^{(1)}=0 \text{ at } r=0, \frac{\partial {u_p}^{(1)}}{\partial r} \text{ at } r=0, \quad (4.39)$$

The analytical results can be expressed in terms of time-averaged volume flow rate which is defined as $\bar{Q}(x) = \int_0^1 Q(x,t)dt$, with the volume flow rate as

$$Q(x,t) = Q_f(x,t) + Q_p(x,t), \tag{4.40}$$

where $Q_f(x,t) = 2\int_0^h (1-C)ru_f dr$ and $Q_p(x,t) = 2\int_0^h Cru_p dr$ stand respectively for the instantaneous volume flow rates for the fluid and particle phases. Due to involving lengthy expressions, it is a boring job. Therefore, we use the transformations from the unsteady laboratory frame to steady wave frame to escape the complexities for this purpose only. And rest of the analyses will be later, from the next section onwards, carried out once again in the unsteady laboratory frame.

In the non-dimensional form, the wave frame and laboratory frame parameters are given by

$$\begin{aligned} &X = x - t,\ R = r,\ U_i(R,X) = u_i(r,x,t) - 1, \\ &V_i(R,X) = v_i(x,r,t),\ q = Q(x,t) - h^2. \end{aligned} \tag{4.41}$$

where (R,X), (U_i,V_i) and q denote respectively the coordinate system, the velocity field $(i = f,p)$ and the flow rate in the wave frame.

In view of equation (4.41), $\tilde{Q}(x) = q + \int_0^1 h^2 dt$, and hence

$$q = Q(x,t) - h^2 = \bar{Q}(x) - 1 + \phi e^{\omega x} - \frac{3}{8}\phi^2 e^{2\omega x} \tag{4.42}$$

For the volume flow rate Q and time-averaged volume rate $\tilde{Q}$, the regular perturbation expansions are as

$$Q = Q^{(0)} + \delta Q^{(1)} + \delta^2 Q^{(2)} + o(\delta^3),$$
$$\tilde{Q} = \tilde{Q}^{(0)} + \delta \tilde{Q}^{(1)} + \delta^2 \tilde{Q}^{(2)} + o(\delta^3),$$

4.3.1 Solution for the zeroth order system

Equation (4.24) is integrated with respect to r in view of equation (4.23), under the first boundary condition of equation (4.25) to get

$$\frac{\partial {u_f}^{(0)}}{\partial r} = \frac{1}{2} r \frac{\partial p^{(0)}}{\partial x},$$

which, on performing integration once more with respect to r under the second boundary condition of equation (4.25), gives

$${u_f}^{(0)} = \frac{1}{4} \frac{\partial p^{(0)}}{\partial x} (r^2 - h^2), \tag{4.43}$$

Continuity equation (4.22) together with equation (4.43) under the third boundary condition of equation (4.25) yields

$$v_f(0) = \frac{r}{16} \{4h \frac{\partial h}{\partial x} \frac{\partial p^{(0)}}{\partial x} - \frac{\partial^2 p^{(0)}}{\partial x^2} (r^2 - 2h^2)\}. \tag{4.44}$$

Now the fourth boundary condition of (4.25) used in equation (4.44) gives

$$\frac{\partial h}{\partial t} = \frac{h^3}{16}\frac{\partial^2 p^{(0)}}{\partial x^2} + \frac{h^2}{4}\frac{\partial h}{\partial x}\frac{\partial p^{(0)}}{\partial x},$$

The zeroth order pressure gradient is derived as

$$\frac{\partial p^{(0)}}{\partial x} = \frac{G(t) + 16\int_0^x h(s,t)\frac{\partial h(s,t)}{\partial t}ds}{h^4}, \tag{4.45}$$

where $G(t)$ is an arbitrary function of t.

Therefore, the zeroth order pressure is given by

$$p^{(0)}(x,t) = p^{(0)}(0,t) + \int_0^x \frac{G(t) + 16\int_0^{x_1} h(s,t)\frac{\partial h(s,t)}{\partial t}ds}{h^4(x_1,t)}dx_1. \tag{4.46}$$

The arbitrary function $G(t)$ for $x = l$ in equation (4.46) is obtained as

$$G(t) = \frac{\{p^0(l,t) - p^0(0,t)\} - 16\int_0^l \frac{\int_0^{x_1} h(s,t)\frac{\partial h(s,t)}{\partial t}ds}{h^4(x_1,t)}dx_1}{\int_0^l \frac{1}{h^4(x_1,t)}dx_1} \tag{4.47}$$

Also, the zeroth order flow rate, in view of equation (4.40), may be

$$Q^{(0)} = {Q_f}^{(0)} = 2\int_0^h r{u_f}^{(0)}dr + 0 = -\frac{1}{8}\frac{\partial p^{(0)}}{\partial x}h^4.$$

which, in view of equation (4.42), is

$$Q^{(0)} = \bar{Q}^{(0)} - 1 + \phi e^{\omega x} - \frac{3}{8}\phi^2 e^{2\omega x} + h^2.$$

Therefore

$$\frac{\partial p^{(0)}}{\partial x} = -8\left\{\frac{\bar{Q}^{(0)} - 1 + \phi e^{\omega x} - \frac{3}{8}\phi^2 e^{2\omega x} + h^2}{h^4}\right\} = P_0 \ (Say) \tag{4.48}$$

Hence, the zeroth order axial and radial velocities of the fluid, in terms of the zeroth order time-averaged volume flow rate, in view of equations (4.43), (4.44) and (4.48), are

$$u_f{}^0 = \frac{1}{4}P_0(r^2 - h^2). \tag{4.49}$$

$$v_f{}^{(0)} = \frac{r}{16}\{4hP_0\frac{\partial h}{\partial x} - \frac{\partial P_0}{\partial x}(r^2 - 2h^2)\}. \tag{4.50}$$

4.3.2 Solution of the first-order system

Equations (4.31) and (4.49) yield the zeroth order axial velocity of the solid particles as

$$u_p{}^{(0)} = \frac{1}{4}\left(r^2 - h^2 - \frac{4}{M}\right)P_0. \tag{4.51}$$

Continuity equation (4.29) is integrated together with equation (4.51) with respect to r under the first boundary condition of equation (4.32) to get the zeroth order radial velocity of the particles as

$$v_p{}^{(0)} = \frac{r}{16}\{4P_0h\frac{\partial h}{\partial x} - \frac{P_0}{\partial x}(r^2 - 2h^2 - \frac{8}{M})\}. \tag{4.52}$$

Equations (4.26) - (4.28) of the first-order system are solved in the similar way to obtain the axial and radial velocities of the fluid of the first-order system as

$$u_f{}^{(1)} = N_1(r^6 - h^6) + N_2(r^4 - h^4) + \left(N_3 + \frac{P_1 + C^{(1)}P_0}{4}\right)(r^2 - h^2). \tag{4.53}$$

$$\begin{aligned} v_f{}^{(1)} = -\frac{1}{8}\frac{\partial N_1}{\partial \partial x}(r^7 - 4h^6 r) - \frac{1}{6}\frac{\partial N_2}{\partial x}(r^5 - 3rh^4) - \frac{1}{4}\Big(\frac{\partial N_3}{\partial x} + \frac{1}{4}\frac{\partial P_{(1)}}{\partial x} \\ + \frac{C^{(1)}}{4}\frac{\partial P_0}{\partial x}\Big)(r^3 - 2rh^2) + \frac{1}{4}(12N_1 + 8N_2h^3 + 2N_3h \\ + P_1h + P_0hC^{(1)})\frac{\partial h}{\partial x}r. \end{aligned} \tag{4.54}$$

where P_1, N_1, N_2 and N_3 are

$$P_1 = \frac{\partial P^{(1)}}{\partial x} = -6N_1h^4 - \frac{16}{3}N_2h^2 - 4N_3 - \frac{P_0}{h^2}C^{(1)}\left(h^2 + \frac{8}{M}\right) - \frac{8\bar{Q}^{(1)}}{h^4}. \tag{4.55}$$

$$N_1 = \frac{Rr_0}{1152}P_0\frac{\partial P_0}{\partial x}. \tag{4.56}$$

$$N_2 = \frac{Rr_0}{1152}\left(16\frac{\partial P_0}{\partial x} - 3P_0\frac{\partial P_0}{\partial x}h^2\right). \tag{4.57}$$

$$N_3 = Re_0\bigg(-\frac{h^2}{16}\frac{\partial P_0}{\partial t} - \frac{P_0}{8}\frac{\partial h}{\partial t}h + \frac{P_0}{64}\frac{\partial P_0}{\partial x}h^4 + \frac{{p_0}^2h^3}{32}\frac{\partial h}{\partial x}\bigg). \tag{4.58}$$

and

$$\bar{Q}^{(1)} = Q^{(1)} = -\frac{3}{4}N_1h^8 - \frac{2}{3}N_2h^6 - \bigg(\frac{N_3}{2} + \frac{1}{8}\frac{\partial P^{(1)}}{\partial x}\frac{P_0}{8}C^{(1)}\bigg)h^4 - \frac{P_0}{M}C^{(1)}h^2.$$

4.3.3 Solution for the second-order system

In this section too, first of all we will formulate the particulate phase velocity of the first order which requires some of the second order equations. Using the equations ((4.51) - (4.53)) in equation (4.38), the axial velocity of the solid particles of the second-order system is given by

$$\begin{aligned}{u_p}^{(1)} = {} & N_1(r^6 - h^6) + N_2(r^4 - h^4) - \frac{\rho Re_0P_0}{32M}\frac{\partial P_0}{\partial x}(r^4 + h^4) + \bigg\{N_3 + \frac{P_1 + C^{(1)}P_0}{4} - \\ & \frac{\rho Re_0}{8M}(2\frac{\partial P_0}{\partial t} - \frac{4P_0}{M}\frac{\partial P_0}{\partial x} - {P_0}^2h\frac{\partial h}{\partial x})\bigg\}(r^2 - h^2) + \frac{\rho Re_0P_0}{16M}\frac{\partial P_0}{\partial x}r^2h^2 \\ & - \frac{\rho Re_0P_0}{8}\bigg\{P_0(r^2 + \frac{4}{M})h\frac{\partial h}{\partial x} + \frac{1}{4}\frac{\partial h}{\partial x}(r^2(h^2 + \frac{8}{M}) + \frac{32}{M})\bigg\} - \frac{P_1}{M} - \frac{5}{2M}C^{(1)}P_0. \end{aligned} \tag{4.59}$$

Further, equation (4.36), in view of (4.59), under the fifth boundary condition (4.39), is solved to get the second order radial velocity of the solid particles as

$$
\begin{aligned}
{v_p}^{(1)} = &-\frac{1}{8}\frac{\partial N_1}{\partial x}\left(r^7-4rh^6\right)-\frac{1}{6}\frac{\partial N_2}{\partial x}\left(r^5-3rh^4\right)+3N_1rh^5\frac{\partial h}{\partial x}+2N_2rh^3\frac{\partial h}{\partial x}\\
&+\left(\frac{\rho Re_0P_0}{192M}\frac{\partial^2P_0}{\partial x^2}+\frac{\rho Re_0}{192M}\left(\frac{\partial P_0}{\partial x}\right)^2\right)\left(r^5+3rh^4-3r^3h^2\right)-\left(\frac{\rho Re_0P_0}{192M}\frac{\partial^2P_0}{\partial x^2}\right.\\
&\left.+\frac{\rho Re_0}{192M}\left(\frac{\partial P_0}{\partial x}\right)^2\right)\left(r^3-2rh^2\right)+\left(\frac{P_1}{4}+\frac{\rho Re_0P_0}{2M^2}\frac{\partial P_0}{\partial x}+\frac{\rho Re_0P_0}{2M}\frac{\partial P_0}{\partial x}\right)rh\frac{\partial h}{\partial x}\\
&+\frac{\rho Re_0P_0}{2M}\left(\frac{\partial h}{\partial x}\right)^2r-\frac{\rho Re_0P_0}{32M}\frac{\partial P_0}{\partial x}\frac{\partial h}{\partial x}r^3h-\frac{C^{(1)}}{16}\frac{\partial P_0}{\partial x}r^3-\frac{1}{16}\frac{\partial P_1}{\partial x}r^3+\frac{1}{2M}\frac{\partial P_1}{\partial x}r\\
&+\frac{5C^{(1)}}{4M}\frac{\partial P_0}{\partial r}r+\left(\frac{3\rho Re_0P_0}{16M}\frac{\partial P_0}{\partial x}\frac{\partial h}{\partial x}+\frac{\rho Re_0{P_0}^2}{16M}\frac{\partial^2h}{\partial x^2}\right)rh^3+\left(\frac{\rho Re_0{P_0}^2}{16M}\left(\frac{\partial h}{\partial x}\right)^2\right.\\
&\left.+\frac{1}{8}\frac{\partial P_1}{\partial x}\right)rh^2+\frac{\rho Re_0P_0}{4M}\frac{\partial^2h}{\partial x^2}rh+\left(\frac{\rho Re_0}{16M}\frac{\partial^2P_0}{\partial x^2}+\frac{\rho Re_0P_0}{32}\left(\frac{\partial h}{\partial x}\right)^2-\frac{1}{4}\frac{\partial N_3}{\partial x}\right.\\
&\left.-\frac{\rho Re_0}{16M}\frac{\partial}{\partial x}\left(\frac{\partial P_0}{\partial t}\right)-\frac{\rho Re_0{P_0}^2}{32M}\left(\frac{\partial h}{\partial x}\right)^2\right)r^3+\frac{\rho Re_0}{128}\frac{\partial^2P_0}{\partial x^2}r^3h^2+\left(\frac{\rho Re_0P_0}{16}\frac{\partial P_0}{\partial x}\frac{\partial h}{\partial x}\right.\\
&\left.+\frac{\rho Re_0P_0}{32}\frac{\partial^2h}{\partial x^2}+\frac{\rho Re_0}{64}\frac{\partial P_0}{\partial x}\frac{\partial h}{\partial x}-\frac{\rho Re_0P_0}{16M}\frac{\partial P_0}{\partial x}\frac{\partial h}{\partial x}-\frac{\rho Re_0{P_0}^2}{32M}\frac{\partial^2h}{\partial x^2}\right)r^3h+\left(N_3\frac{\partial h}{\partial x}\right.\\
&\left.+\frac{C^{(1)}P_0}{4}\frac{\partial h}{\partial x}-\frac{\rho Re_0}{8M}\frac{\partial P_0}{\partial t}\frac{\partial h}{\partial x}\right)rh+\left(\frac{\rho Re_0{P_0}^2}{8M}\left(\frac{\partial h}{\partial x}\right)^2\right.\\
&\left.+\frac{1}{2}\frac{\partial N_3}{\partial x}+\frac{C^{(1)}}{8}\frac{\partial P_0}{\partial x}-\frac{\rho Re_0}{8M}\frac{\partial}{\partial x}\left(\frac{\partial P_0}{\partial t}\right)\right)rh^2. \qquad (4.60)
\end{aligned}
$$

The second order axial velocity of the fluid is derived from equation (4.35) by using equations (4.49), (4.53) and (4.59) under the second boundary condition of equation (4.39), as

$$
\begin{aligned}
{u_f}^{(2)} = &\alpha_1\left(r^{10}-h^{10}\right)+\alpha_2\left(r^8-h^8\right)+\alpha_3\left(r^6-h^6\right)+\alpha_4\left(r^4-h^4\right)\\
&+\alpha_5\left(r^2-h^2\right)+\frac{1}{8}\left(2P_2-3C^{(1)}P_1-6{C^{(1)}}^2P_0-12C^{(1)}N_3\right)\left(r^2-h^2\right). \qquad (4.61)
\end{aligned}
$$

And then using (4.61) in equation (4.33) under the boundary condition (4.39), the second-order radial velocity is given by

$$\begin{aligned} {v_f}^{(2)} = &-\frac{1}{12}\frac{\partial \alpha_1}{\partial x}\left(r^{11}-6rh^{10}\right)-\frac{1}{10}\frac{\partial \alpha_2}{\partial x}\left(r^{9}-5rh^{8}\right)-\frac{1}{8}\frac{\partial \alpha_3}{\partial x}\left(r^{7}-4rh^{6}\right)\\ &-\frac{1}{6}\frac{\partial \alpha_4}{\partial x}\left(r^{5}-3rh^{4}\right)-\frac{1}{4}\frac{\partial \alpha_5}{\partial x}\left(r^{3}-2rh^{2}\right)+5\alpha_1 h^9\frac{\partial h}{\partial x}r+4\alpha_2 h^7\frac{\partial h}{\partial x}r\\ &+3\alpha_3 h^5\frac{\partial h}{\partial x}r+2\alpha_4 h^3\frac{\partial h}{\partial x}r+\alpha_5 h\frac{\partial h}{\partial x}r+\frac{1}{32}\Bigg(2\frac{\partial P_2}{\partial x}-3C^{(1)}\frac{\partial P_1}{\partial x}\\ &-6{C^{(1)}}^2\frac{\partial P_0}{\partial x}-12C^{(1)}\frac{\partial N_3}{\partial x}\Bigg)\left(2rh^2-r^3\right)+\Bigg(2P_2-3C^{(1)}P_1-6{C^{(1)}}^2P_0\\ &-12C^{(1)}N_3\Bigg)\frac{h}{8}\frac{\partial h}{\partial x}r+\frac{3C^{(1)}}{16}\frac{\partial N_1}{\partial x}\left(r^{7}-4rh^{6}\right)+\frac{3C^{(1)}}{12}\frac{\partial N_2}{\partial x}\left(r^{5}-3rh^{4}\right)\\ &-\frac{9}{2}N_1C^{(1)}h^5\frac{\partial h}{\partial x}r-3N_2C^{(1)}h^3\frac{\partial h}{\partial x}r. \end{aligned} \tag{4.62}$$

where

$$\begin{aligned} P_2=\frac{\partial p^{(2)}}{\partial x}=&\frac{3}{2}C^{(1)}P_1+3{C^{(1)}}^2P_0+6C^{(1)}N_3-4\alpha_5+\frac{2\rho Re_0}{M}\Bigg(\frac{\partial P_0}{\partial t}-\frac{2P_0}{M}\frac{\partial P_0}{\partial x}\\ &+\frac{2}{M}\frac{\partial P_0}{\partial x}\Bigg)-\frac{8C^{(1)}}{h^2M}\left(P_1+\frac{5}{2}P_0C^{(1)}+\rho Re_0P_0\frac{\partial P_0}{\partial x}\right)+\Bigg\{8C^{(1)}N_2-\frac{16}{3}\alpha_4\\ &+C^{(1)}\left(1-\frac{\rho Re_0P_0}{12M}\right)\frac{\partial P_0}{\partial x}\Bigg\}h^2-6\alpha_3h^4+\left(9C^{(1)}N_1-\frac{32}{5}\alpha_2\right)h^6\\ &-\frac{\rho Re_0{P_0}^2C^{(1)}}{2M}h\frac{\partial h}{\partial x}-10\alpha_1h^8-8\frac{\tilde{Q}^{(2)}}{h^4}. \end{aligned} \tag{4.63}$$

$$\alpha_1=Re_0\left(\frac{N_1}{400}\frac{\partial P_0}{\partial x}-\frac{3P_0}{1600}\frac{\partial N_1}{\partial x}\right),$$

$$\alpha_2 = Re_0\left\{\frac{P_0N_1}{64}\frac{\partial h}{\partial x}h-\left(\frac{N_1}{256}\frac{\partial P_0}{\partial x}+\frac{P_0}{256}\frac{\partial N_1}{\partial x}\right)h^2+\frac{N_2}{256}\frac{\partial P_0}{\partial x}+\frac{2P_0}{768}\frac{\partial N_2}{\partial x}\right\},$$

$$\begin{aligned}\alpha_3 = Re_0\Bigg\{&\frac{P_0N_2h}{72}\frac{\partial h}{\partial x}-\frac{N_2h^2}{144}\frac{\partial P_0}{\partial x}+\frac{N_3}{36}+\frac{P_1+C^{(1)}P_0}{72}\\&+\frac{P_0}{288}\left(\frac{\partial N_3}{\partial x}+\frac{3}{4}\frac{\partial P_1}{\partial x}+\frac{3C^{(1)}}{4}\frac{\partial P_0}{\partial x}\right)-\frac{P_0h^2}{144}\frac{\partial N_2}{\partial x}+\frac{C^{(1)}P_0}{5760}\frac{\partial P_0}{\partial x}\\&+\frac{C^{(1)}\rho P_0}{1152}\frac{\partial P_0}{\partial x}\Bigg\},\end{aligned}$$

$$\begin{aligned}\alpha_4 = Re_0\Bigg\{&\frac{1}{64}\frac{\partial P_0}{\partial t}-\frac{N_1h^6}{64}\frac{\partial P_0}{\partial x}-\frac{N_2h^4}{64}\frac{\partial P_0}{\partial x}-\frac{h^2}{8}\Bigg(N_3\\&+\frac{P_1+C^{(1)}P_0}{2}\Bigg)-\frac{P_0h^2}{64}\left(\frac{\partial N_3}{\partial x}+\frac{3}{4}\frac{\partial P_1}{\partial x}+\frac{3C^{(1)}}{4}\frac{\partial P_0}{\partial x}\right)\\&+\frac{P_0}{128}\frac{\partial h}{\partial x}\Big(12N_1+8N_2h^3+2N_3h+P_1h+P_0hC^{(1)}\Big)\\&-\frac{P_0h^6}{64}\frac{\partial N_1}{\partial x}-\frac{3P_0N_1h^5}{32}\frac{\partial h}{\partial x}-\frac{P_0h^3N_2}{16}\frac{\partial h}{\partial x}\Bigg\},\end{aligned}$$

$$\alpha_5 = Re_0\Big\{-\frac{h^2}{16}\frac{\partial P_0}{\partial t}-\frac{P_0 h}{8}\frac{\partial h}{\partial t}+\frac{N_1 h^8}{16}\frac{\partial P_0}{\partial x}+\frac{N_2 h^6}{16}\frac{\partial P_0}{\partial x}$$
$$+\frac{h^4}{4}\left(N_3+\frac{P_1+C^{(1)}P_0}{2}\right)+\frac{N_1 P_0 h^7}{2}\frac{\partial h}{\partial x}+\frac{3N_2 P_0 h^5}{8}\frac{\partial h}{\partial x}+\frac{P_0 h^8}{16}$$
$$\frac{\partial N_1}{\partial x}+\frac{P_0 h^6}{16}\frac{\partial N_2}{\partial x}+\frac{P_0 h^4}{16}\left(\frac{\partial N_3}{\partial x}+\frac{1}{2}\frac{\partial P_1}{\partial x}+\frac{C^{(1)}}{2}\frac{\partial P_0}{\partial x}\right)+\frac{C^{(1)}h^2}{16}\frac{\partial P_0}{\partial t}$$
$$+\frac{C^{(1)}P_0 h}{8}\frac{\partial h}{\partial t}+\frac{P_0 h^4}{64}\frac{\partial P_0}{\partial x}-\frac{{P_0}^2 h^3}{32}\frac{\partial h}{\partial x}-\frac{C^{(1)}\rho h^2}{32}\Big(2\frac{\partial P_0}{\partial t}-\frac{4P_0}{M}\frac{\partial P_0}{\partial x}$$
$$-{P_0}^2 h\frac{\partial h}{\partial x}\Big)-\frac{C^{(1)}\rho {P_0} h^4}{128}\frac{\partial P_0}{\partial x}+\frac{2C^{(1)}P_1+5{C^{(1)}}^3 P_0}{4}+\frac{\rho {P_0}^2 h}{8}\frac{\partial h}{\partial x}+2C^{(1)}\frac{\partial P_0}{\partial x}\Big\}.$$

and

$$\tilde{Q}^{(2)} = Q^{(2)} = \frac{h^4}{8}\Big[\frac{3}{2}C^{(1)}P_1+3{C^{(1)}}^2 P_0+6C^{(1)}N_3-4\alpha_5+\frac{2\rho Re_0}{M}\Big(\frac{\partial P_0}{\partial t}$$
$$-\frac{2P_0}{M}\frac{\partial P_0}{\partial x}+\frac{2}{M}\frac{\partial P_0}{\partial x}\Big)\Big]-\frac{C^{(1)}}{M}\left(P_1+\frac{5}{2}P_0 C^{(1)}+\rho Re_0 P_0\frac{\partial P_0}{\partial x}\right)h^2$$
$$+\left\{C^{(1)}N_2-\frac{2}{3}\alpha_4+\frac{C^{(1)}}{8}\left(1-\frac{\rho Re_0 P_0}{12M}\right)\frac{\partial P_0}{\partial x}\right\}h^6-\frac{3}{4}\alpha_3 h^8+\Big(\frac{9}{8}C^{(1)}N_1$$
$$-\frac{4}{5}\alpha_2\Big)h^{10}-\frac{\rho Re_0 {P_0}^2 C^{(1)}}{16M}\frac{\partial h}{\partial x}h^5-\frac{5}{4}\alpha_1 h^{12}-\frac{P_2}{8}h^4. \quad (4.64)$$

The solutions given in equations (4.17) - (4.21) together constitute the required results for the fluid and particulate velocities, and the pressure gradient in terms of time-averaged volume flow rate. Therefore, the axial and radial velocities of the fluid in the fixed frame, and the pressure gradient are as follows:

$$u_f = \frac{P_0}{4}\left(r^2-h^2\right)+\delta\Big\{N_1\left(r^6-h^6\right)+N_2\left(r^4-h^4\right)+\left(N_3+\frac{P_1+C^{(1)}P_0}{4}\right)\left(r^2-h^2\right)\Big\}+\delta^2\Big\{\alpha_1\left(r^{10}-h^{10}\right)+\alpha_2\left(r^8-h^8\right)+\alpha_3\left(r^6-h^6\right)+\alpha_4\left(r^4-h^4\right)+\alpha_5\left(r^2-h^2\right)+\left(\frac{2P_2-3C^{(1)}P_1-6{C^{(1)}}^2P_0-12C^{(1)}N_3}{8}\right)\left(r^2-h^2\right)\Big\}. \quad (4.65)$$

$$v_f = \frac{r}{4}\Big\{h\frac{\partial h}{\partial x}P_0-\frac{\partial P_0}{\partial x}\left(\frac{r^2}{4}-\frac{h^2}{2}\right)\Big\}+\delta\Big\{-\frac{1}{8}\frac{\partial N_1}{\partial x}\left(r^7-4h^6r\right)-\frac{1}{6}\frac{\partial N_2}{\partial x}\Big(r^5-3rh^4\Big)-\frac{1}{4}\left(\frac{\partial N_3}{\partial x}+\frac{1}{4}\frac{\partial P_1}{\partial x}+\frac{C^{(1)}}{4}\frac{\partial P_0}{\partial x}\right)\left(r^3-2rh^2\right)+\frac{1}{4}\Big(12N_1+8N_2h^3+2N_3h+P_1h+P_0hC^{(1)}\Big)\frac{\partial h}{\partial x}r\Big\}+\delta^2\Big\{-\frac{1}{12}\frac{\partial\alpha_1}{\partial x}\left(r^{11}-6rh^{10}\right)-\frac{1}{10}\frac{\partial\alpha_2}{\partial x}\Big(r^9-5rh^8\Big)-\frac{1}{8}\frac{\partial\alpha_3}{\partial x}\left(r^7-4rh^6\right)-\frac{1}{6}\frac{\partial\alpha_4}{\partial x}\left(r^5-3rh^4\right)-\frac{1}{4}\frac{\partial\alpha_5}{\partial x}\left(r^3-2rh^2\right)+5\alpha_1h^9\frac{\partial h}{\partial x}r+4\alpha_2h^7\frac{\partial h}{\partial x}r+3\alpha_3h^5\frac{\partial h}{\partial x}r+2\alpha_4h^3\frac{\partial h}{\partial x}r+\alpha_5h\frac{\partial h}{\partial x}r+\frac{1}{32}\Big(2\frac{\partial P_2}{\partial x}-3C^{(1)}\frac{\partial P_1}{\partial x}-6{C^{(1)}}^2\frac{\partial P_0}{\partial x}-12C^{(1)}\frac{\partial N_3}{\partial x}\Big)\left(2rh^2-r^3\right)+\Big(2P_2-3C^{(1)}P_1-6{C^{(1)}}^2P_0-12C^{(1)}N_3\Big)\frac{h}{8}\frac{\partial h}{\partial x}r+\frac{3C^{(1)}}{16}\frac{\partial N_1}{\partial x}\left(r^7-4rh^6\right)+\frac{3C^{(1)}}{12}\frac{\partial N_2}{\partial x}\Big(r^5-3rh^4\Big)-\frac{9}{2}N_1C^{(1)}h^5\frac{\partial h}{\partial x}r-3N_2C^{(1)}h^3\frac{\partial h}{\partial x}r\Big\}. \quad (4.66)$$

$$u_p = \frac{1}{4}\left(r^2 - h^2 - \frac{4}{M}\right)P_0 + \delta\Big[N_1\left(r^6 - h^6\right) + N_2\left(r^4 - h^4\right) - \frac{\rho Re_0 P_0}{32M}\frac{\partial P_0}{\partial x}$$
$$\left(r^4 + h^4\right) + \left\{N_3 + \frac{P_1 + C^{(1)}P_0}{4} - \frac{\rho Re_0}{8M}\left(2\frac{\partial P_0}{\partial t} - \frac{4P_0}{M}\frac{\partial P_0}{\partial x} - P_0^2 h\frac{\partial h}{\partial x}\right)\right\}\left(r^2\right.$$
$$\left. - h^2\right) + \frac{\rho Re_0 P_0}{16M}\frac{\partial P_0}{\partial x}r^2h^2 - \frac{\rho Re_0 P_0}{8}\left\{P_0 h\left(r^2 + \frac{4}{M}\right)\frac{\partial h}{\partial x} + \frac{1}{4}\frac{\partial P_0}{\partial x}\left(r^2\left(h^2\right.\right.\right.$$
$$\left.\left.\left. + \frac{8}{M}\right) + \frac{32}{M}\right)\right\} - \frac{P_1}{M} - \frac{5}{2M}C^{(1)}P_0\Big]. \quad (4.67)$$

$$v_p = \frac{r}{16}\left\{4P_0 h\frac{\partial h}{\partial x} - \frac{\partial P_0}{\partial x}\left(r^2 - 2h^2 - \frac{8}{M}\right)\right\} + \delta\Big\{-\frac{1}{8}\frac{\partial N_1}{\partial x}\left(r^7 - 4rh^6\right)$$
$$-\frac{1}{6}\frac{\partial N_2}{\partial x}\left(r^5 - 3rh^4\right) + 3N_1 rh^5\frac{\partial h}{\partial x} + 2N_2 rh^3\frac{\partial h}{\partial x} + \left(\frac{\rho Re_0 P_0}{192M}\frac{\partial^2 P_0}{\partial x^2} + \frac{\rho Re_0}{192M}\left(\frac{\partial P_0}{\partial x}\right)^2\right)$$
$$\left(r^5 + 3rh^4 - 3r^3h^2\right) - \left(\frac{\rho Re_0 P_0}{192M}\frac{\partial^2 P_0}{\partial x^2} + \frac{\rho Re_0}{192M}\left(\frac{\partial P_0}{\partial x}\right)^2\right)\left(r^3 - 2rh^2\right) + \left(\frac{P_1}{4}\right.$$
$$\left. + \frac{\rho Re_0 P_0}{2M^2}\frac{\partial P_0}{\partial x} + \frac{\rho Re_0 P_0}{2M}\frac{\partial P_0}{\partial x}\right)rh\frac{\partial h}{\partial x} + \frac{\rho Re_0 P_0}{2M}\left(\frac{\partial h}{\partial x}\right)^2 r - \frac{\rho Re_0 P_0}{32M}\frac{\partial P_0}{\partial x}\frac{\partial h}{\partial x}r^3h$$
$$-\frac{C^{(1)}}{16}\frac{\partial P_0}{\partial x}r^3 - \frac{1}{16}\frac{\partial P_1}{\partial x}r^3 + \frac{1}{2M}\frac{\partial P_1}{\partial x}r + \frac{5C^{(1)}}{4M}\frac{\partial P_0}{\partial r}r + \left(\frac{3\rho Re_0 P_0}{16M}\frac{\partial P_0}{\partial x}\frac{\partial h}{\partial x}\right.$$
$$\left. + \frac{\rho Re_0 {P_0}^2}{16M}\frac{\partial^2 h}{\partial x^2}\right)rh^3 + \left(\frac{\rho Re_0 {P_0}^2}{16M}\left(\frac{\partial h}{\partial x}\right)^2 + \frac{1}{8}\frac{\partial P_1}{\partial x}\right)rh^2 + \frac{\rho Re_0 P_0}{4M}\frac{\partial^2 h}{\partial x^2}rh +$$
$$\left(\frac{\rho Re_0}{16M}\frac{\partial^2 P_0}{\partial x^2} + \frac{\rho Re_0 P_0}{32}\left(\frac{\partial h}{\partial x}\right)^2 - \frac{1}{4}\frac{\partial N_3}{\partial x} - \frac{\rho Re_0}{16M}\frac{\partial}{\partial x}\left(\frac{\partial P_0}{\partial t}\right)\right.$$
$$\left. - \frac{\rho Re_0 {P_0}^2}{32M}\left(\frac{\partial h}{\partial x}\right)^2\right)r^3 + \frac{\rho Re_0}{128}\frac{\partial^2 P_0}{\partial x^2}r^3h^2 + \left(\frac{\rho Re_0 P_0}{16}\frac{\partial P_0}{\partial x}\frac{\partial h}{\partial x} + \frac{\rho Re_0 P_0}{32}\frac{\partial^2 h}{\partial x^2}\right.$$
$$\left. + \frac{\rho Re_0}{64}\frac{\partial P_0}{\partial x}\frac{\partial h}{\partial x} - \frac{\rho Re_0 P_0}{16M}\frac{\partial P_0}{\partial x}\frac{\partial h}{\partial x} - \frac{\rho Re_0 {P_0}^2}{32M}\frac{\partial^2 h}{\partial x^2}\right)r^3h + \left(N_3\frac{\partial h}{\partial x} + \frac{C^{(1)}P_0}{4}\frac{\partial h}{\partial x}\right.$$
$$\left. - \frac{\rho Re_0}{8M}\frac{\partial P_0}{\partial t}\frac{\partial h}{\partial x}\right)rh + \left(\frac{\rho Re_0 {P_0}^2}{8M}\left(\frac{\partial h}{\partial x}\right)^2 + \frac{1}{2}\frac{\partial N_3}{\partial x} + \frac{C^{(1)}}{8}\frac{\partial P_0}{\partial x} - \frac{\rho Re_0}{8M}\frac{\partial}{\partial x}\left(\frac{\partial P_0}{\partial t}\right)\right)rh^2\Big\}.$$

(4.68)

$$
\begin{aligned}
p = -8\Bigg(\frac{\tilde{Q}^{(0)} - e^{2bx} + \phi\ e^{(b+\omega)x} - \frac{3}{8}\phi^2 e^{2\omega x} + h^2}{h^4}\Bigg) - \delta\Bigg\{6N_1h^4 + \frac{16}{3}N_2h^2 \\
+ 4N_3 - 8C^{(1)}\Bigg(\frac{\tilde{Q}^{(0)} - e^{2bx} + \phi\ e^{(b+\omega)x} - \frac{3}{8}\phi^2 e^{2\omega x} + h^2}{h^6}\Bigg)\Bigg(\frac{8}{M} + h^2\Bigg) + \frac{8\tilde{Q}^{(1)}}{h^4}\Bigg\} \\
+ \delta^2\Bigg\{\frac{3}{2}C^{(1)}P_1 + 3{C^{(1)}}^2P_0 + 6C^{(1)}N_3 - 4\alpha_5 + \frac{2\rho Re_0}{M}\Bigg(\frac{\partial P_0}{\partial t} - \frac{2P_0}{M}\frac{\partial P_0}{\partial x} + \frac{2}{M}\frac{\partial P_0}{\partial x}\Bigg) \\
- \frac{8C^{(1)}}{h^2M}\Bigg(P_1 + \frac{5}{2}P_0C^{(1)} + \rho Re_0P_0\frac{\partial P_0}{\partial x}\Bigg) + \Bigg\{8C^{(1)}N_2 - \frac{16}{3}\alpha_4 + C^{(1)}\Bigg(1 - \frac{\rho Re_0P_0}{12M}\Bigg) \\
\frac{\partial P_0}{\partial x}\Bigg\}h^2 - 6\alpha_3h^4 + \Bigg(9C^{(1)}N_1 - \frac{32}{5}\alpha_2\Bigg)h^6 - \frac{\rho Re_0{P_0}^2C^{(1)}}{2M}h\frac{\partial h}{\partial x} - 10\alpha_1h^8 - 8\frac{\tilde{Q}^{(2)}}{h^4}\Bigg\}.
\end{aligned}
\tag{4.69}
$$

4.3.4 Stream function

The flow patterns of fluid are also given by counters of the constant stream function Ψ_f, in the moving frame defined as

$$d\Psi_f = 2RU_f dR - 2RV_f dX.$$

The stream function $\psi_f(x,r,t)$ in the fixed frame may be achieved by the solution of the exact differential equation $d\psi_f = 2\Big(u_f - 1\Big)rdr - 2v_f rdx$ using the equation (4.41). Therefore the stream function may be achieved by evaluating

$$2\int\left[\frac{P_0}{4}\left(r^2-h^2\right)+\delta\left\{N_1\left(r^6-h^6\right)+N_2\left(r^4-h^4\right)+\left(N_3+\frac{P_1+C^{(1)}P_0}{4}\right)\right.\right.$$
$$\left.\left(r^2-h^2\right)\right\}+\delta^2\left\{\alpha_1\left(r^{10}-h^{10}\right)+\alpha_2\left(r^8-h^8\right)+\alpha_3\left(r^6-h^6\right)+\alpha_4\left(r^4-h^4\right)$$
$$+\alpha_5\left(r^2-h^2\right)+\left(\frac{2P_2-3C^{(1)}P_1-6C^{(1)^2}P_0-12C^{(1)}N_3}{8}\right)\left(r^2-h^2\right)\Big\}-1\Big]rdr,$$

Consequently we have

$$\psi_f(r,x,t)=r^2\Big[\frac{P_0}{8}\left(r^2-2h^2\right)+\delta\Big\{\frac{N_1}{4}\left(r^6-4h^6\right)+\frac{N_2}{3}\left(r^4-3h^4\right)+\frac{1}{8}\Big(4N_3$$
$$+P_1+C^{(1)}P_0\Big)\left(r^2-2h^2\right)\Big\}+\delta^2\Big\{\frac{\alpha_1}{6}\left(r^{10}-6h^{10}\right)+\frac{\alpha_2}{5}\left(r^8-5h^8\right)+\frac{\alpha_3}{4}\Big(r^6$$
$$-4h^6\Big)+\frac{\alpha_4}{3}\left(r^4-3h^4\right)+\frac{\alpha_5}{2}\left(r^2-2h^2\right)$$
$$+\left(\frac{2P_2-3C^{(1)}P_1-6C^{(1)^2}P_0-12C^{(1)}N_3}{16}\right)\left(r^2-2h^2\right)\Big\}-1\Big]. \quad (4.70)$$

For wave number, $\delta \to 0$, equations (4.65) - (4.70) reduce to the corresponding equations derived by Shapiro *et al.* (1969).

4.4 Discussions and Results

This improved version which includes the second order perturbation terms is expected to bring about changes at least in quantitative terms. For application of the analytical formulations presented here, the length and the diameter of the oesophagus based in the literature are considered as 25–30 cm (Lamb and Griffin, 2005) and 1.8 – 2.1 cm (Joohee *et al.*, 2012) respectively. The uniform radii of the

suspended particles are assumed as 0.04 cm. We also consider two boluses in oesophagus at a time while swallowing.

These considerations of oesophagus related dimensions, we evaluated the parameters as $\delta = 0.08$ and $M = 1139$. The analytical results are presented in the fixed frame up to the second order of the time-averaged volume flow rate $\tilde{Q} = \tilde{Q}^0 + \delta\tilde{Q}^1 + \delta^2\tilde{Q}^{(2)}$. Then we wrote codes by putting $\tilde{Q}^{(0)} = \tilde{Q} - \delta\tilde{Q}^1 - \delta^2\tilde{Q}^{(2)}$ in the solutions (4.65) - (4.70) for numerical evaluations. We draw diagrams for the pressure gradient, the axial and radial velocities and the streamlines of the flow. They are shown in Figures 4.2 - 4.8 or various assumed parameters.

The axial velocities of the fluid and the solid particles are displayed in Figures 4.2 for the values $r = 0.3$ and ((4.2a), (4.2b)) $t = 0.0$ ((4.2c), (4.2d)) $t = 0.4$. The diagrams are based on equations (4.59) and (4.65). Other parameters are assumed as $\delta = 0.08$, $k = 0.02$, $C = 0.12$, $\phi = 0.7$, $Re_0 = 5$, $\bar{Q} = 1.5$, $\bar{Q}^{(1)} = 15$, $\bar{Q}^{(2)} = 15$, $M = 1139$. At $t = 0.0$ (Figure (4.2a), (4.2b)) and $t = 0.4$ (Figure (4.2c), (4.2d)) we observe that the fluid axial velocity exceeds particulate axial velocity almost everywhere. But analyzing equations (4.59) and (4.65), we reveal that the fluid does not move at the wall, while the suspended particulate matter moves axially. This indicates that the suspended particles near the tube wall overtake the fluid. In Figures ((4.2c), (4.2d)), it is observed that the axial velocity is negative in the regions in the vicinity of maximum occlusions paving way to instantaneous backward flow. Retrograde motion is observed in a small region with maximum occlusion. This makes the net flow positive. It is further observed that the velocity at the second occlusion point exceeds that at the first occlusion point which is due to dilation of the wave amplitude. Figures ((4.2a), (4.2c)) correspond to the present analysis while Figures ((4.2b), (4.2d)) correspond to Pandey and Singh

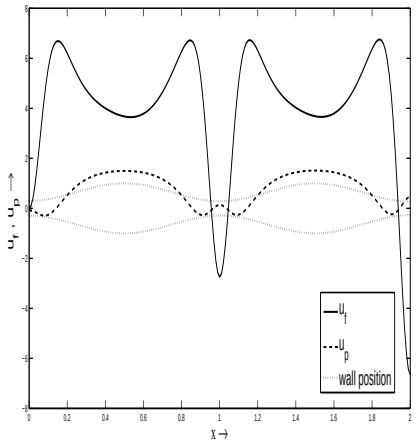

(4.2a) $t = 0.0$

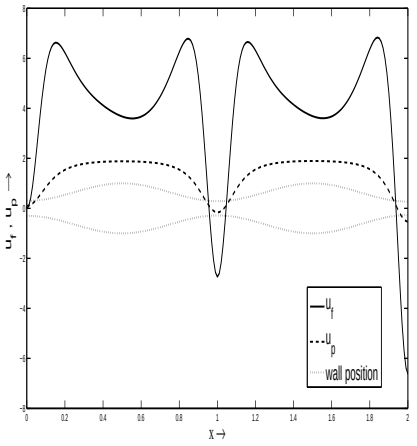

(4.2b) $t = 0.0$

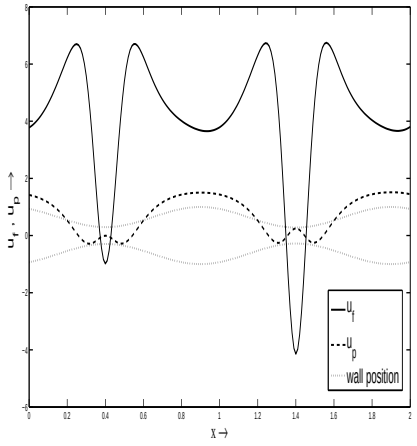

(4.2c) $t = 0.4$

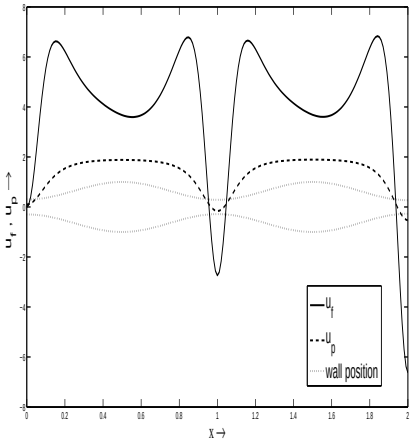

(4.2d) $t = 0.4$

Figure 4.2: (((4.2a), (4.2b)) - ((4.2c), (4.2d))) Axial velocity profile of the fluid and solid particles versus the tube length at the fixed radial distance $r = 0.3$ and ((4.2a), (4.2b)) $t = 0.0$ ((4.2c), (4.2d) $t = 0.4$. Other parameters are taken as $\delta = 0.08$, $\omega = 0.02$, $C = 0.12$, $\phi = 0.7$, $Re_0 = 5$, $\bar{Q} = 1.0$, $\bar{Q}^{(1)} = 15$, $\bar{Q}^{(2)} = 15$, $M = 1139$. ((4.2a), (4.2c)) correspond to the present analysis while ((4.2b), (4.2d)) correspond to the Pandey and Singh, 2018).

(2018) who presented solutions limited to the first order of δ. The quantitative differences are very clear.

Fluid and particulate matter velocities vs. radial distance are plotted in Figures 4.3. It is observed that near the centre of the tube, the fluid velocity

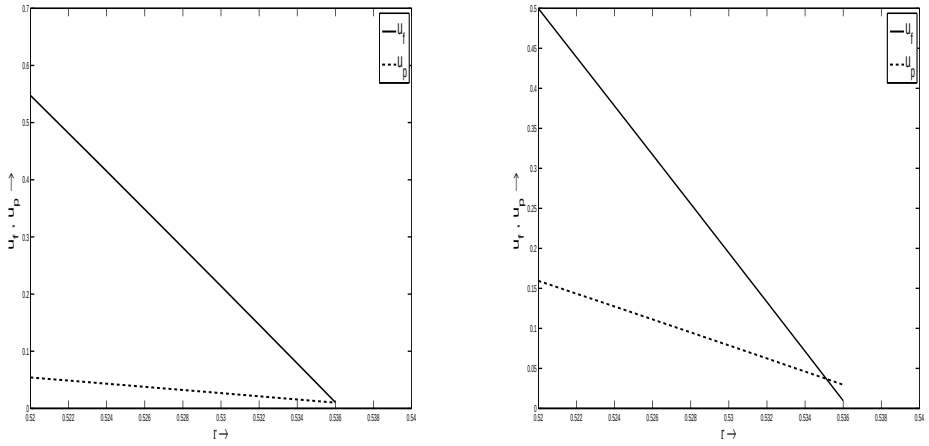

(4.3a) $t = 0.0$ (4.3b) $t = 0.0$

Figure 4.3: The radial profiles of the axial velocity respectively of the fluid and solid particles versus the tube radius at the fixed axial position $x = 0.6$ and $t = 0.4$. Other parameters are taken as $\delta = 0.08$, $\omega = 0.02$, $C = 0.12$, $\phi = 0.7$, $Re_0 = 5$, $\bar{Q} = 1.5$, $\bar{Q}^{(1)} = 20$, $\bar{Q}^{(2)} = 20$, $M = 1139$.

exceeds the particle velocity but as we reach the tube periphery the trend changes with particle velocity exceeding the fluid velocity. Quantitative difference are clear in the plots drawn based on the present analysis and that those based on Pandey and Singh, 2018).

The wave amplitude dilation impacts on the axial velocity are displayed in Figures 4.4 in which the parameters are $\omega = 0.0, 0.05, 0.1$, $x = 0.3$, $t = 0.9$, $\delta = 0.08$, $C = 0.12$, $\phi = 0.7$, $Re_0 = 5$, $\bar{Q} = 1.5$, $\bar{Q}^{(1)} = 20$, $\bar{Q}^{(2)} = 20$, $M = 1139$. We observe that the dilation of the wave amplitude increases the axial velocity at the fixed axial positions for both the fluid and particulate motions. However, the differences in magnitude are obvious between the present analysis plotted in Figures ((4.4a), (4.4c)) and those given by Pandey and Singh (2018) displayed in Figures ((4.4b), (4.4d)).

Figures ((4.5a), (4.5b)) display the effect of the particulate matter concentration ($C = 0.0, 0.16, 0.32$) on the axial velocities of the fluid along the radius

at a specified axial location $x = 0.3$ and at $t = 0.9$ We take the parameters as $\omega = 0.02, \phi = 0.7, Re_0 = 5, \bar{Q}^{(1)} = 20, \bar{Q}^{(2)} = 20$. The diagrams show that the axial fluid velocity falls with increasing volume fraction, i.e., velocity will be less for fluids with particulate suspension. The difference between this analysis, displayed in Figure (4.5a), and that in Pandey and Singh (2018), plotted in Figure (4.5b), is quite significant.

The trend of the radial velocity of the fluid was examined by fixing the axial position at $x = 0.2$ for $t = 0.3$ against different volume fractions ($C = 0.0, 0.16, 0.32$) and displayed in Figures ((4.6a) -(4.6b)). We observe that the velocities corresponding to all volume fractions fall from zero i.e., the move away from the tube wall, reach a minimum (of maximum magnitude) and then once again increase to finally satisfy the boundary condition that it is zero in the middle of the tube i.e., $r = 0$. These curves reflect the wall motion in the transverse direction. Higher the volume fraction of suspended particles, lesser is the magnitude of the radial velocity of the fluid. Figures (4.6a) and (4.6b) respectively display the results obtained in the present analysis and that of Pandey and Singh (2018).

The pressure gradient of the fluid-particle mixture is plotted in Figures ((4.7a)-(4.7b)) against the time-averaged volume flow rate $\bar{Q}$ for volume fractions ($C = 0.0, 0.16, 0.32$) at the fixed axial position and the fixed time. We arbitrarily choose $x = 0.8$ and $t = 0.4$. For qualitative interpretation of the analytical formulation we set parameters as $\omega = 0.02$, $\phi = 0.6$, $Re_0 = 5$, $\bar{Q}^{(1)} = 15$, $\bar{Q}^{(1)} = 15$. A close observation is the pressure gradient generally drops when C increases. This means that concentration of particulate matter in the fluid medium affect the pumping characteristics. It is found that a positive pressure gradient obstructs

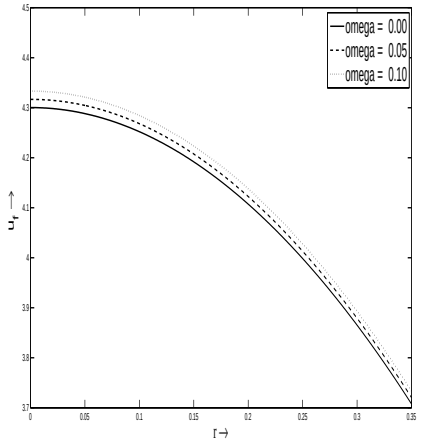

(4.4a)

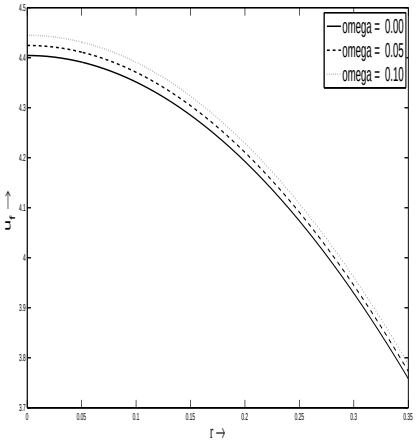

(4.4b)

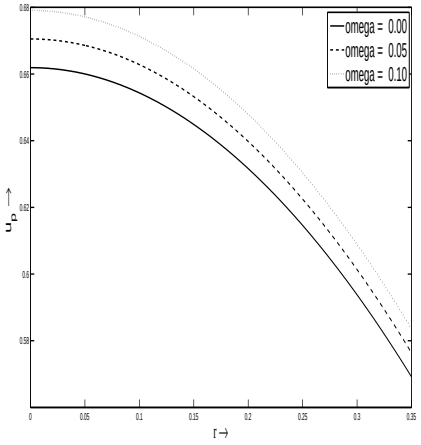

(4.4c)

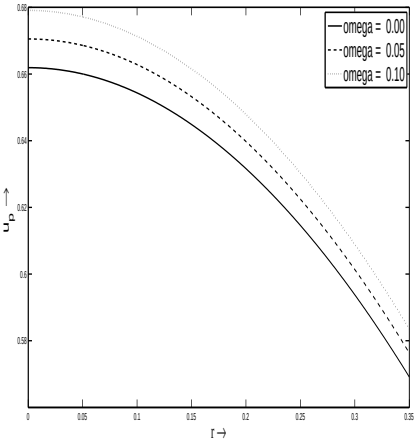

(4.4d)

Figure 4.4: Radial profiles the axial velocity respectively of (4.4a)-(4.4b) the fluid and (4.4c)-(4.4d) solid particles versus the radial distance at the fixed axial position $x = 0.3$ and time $t = 0.9$ showing the impact of amplitude dilation parameter ω. Other parameters are taken as $\delta = 0.08$, $C = 0.12$, $\phi = 0.7$, Re_0, $\bar{Q} = 1.5$, $\bar{Q}^{(1)} = 20$, $\bar{Q}^{(2)} = 20$, $M = 1139$. Solid, dashed and dashed dotted line correspond respectively to $\omega = 0.0$, $\omega = 0.05$ and $\omega = 0.10$. Figures (4.4b)-(4.4d) correspond to Pandey and Singh (2018).

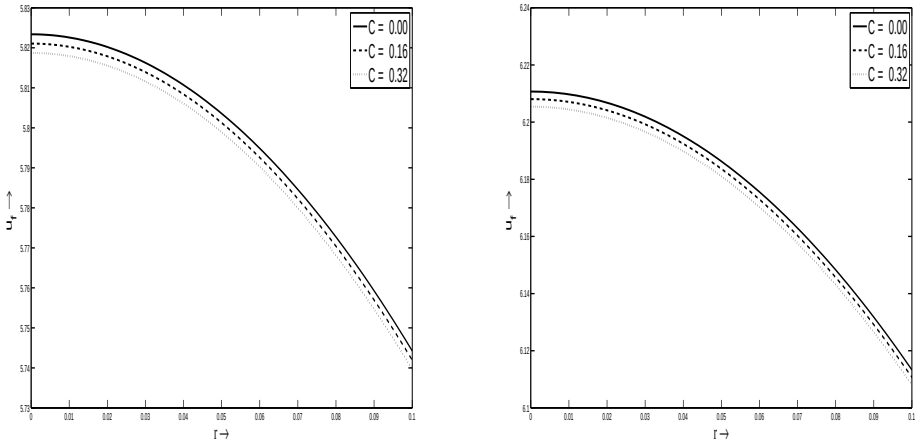

(4.5a) $\delta = 0.08$ (4.5b) $\delta = 0.08$

Figure 4.5: The impact of particulate matter concentration (i.e. the volume fraction C) on the axial velocity of the fluid plotted verses radial distance at the fixed axial position $x = 0.3$ for $\omega = 0.02$, $\phi = 0.8$, $Re_0 = 5$, $\bar{Q} = 1.5$, $\bar{Q}^{(1)} = 20$, $\bar{Q}^{(2)} = 20$, $t = 0.9$, $M = 1139$, (4.5*a*)$\delta = 0.08$, (4.5*b*)$\delta = 0.08$.

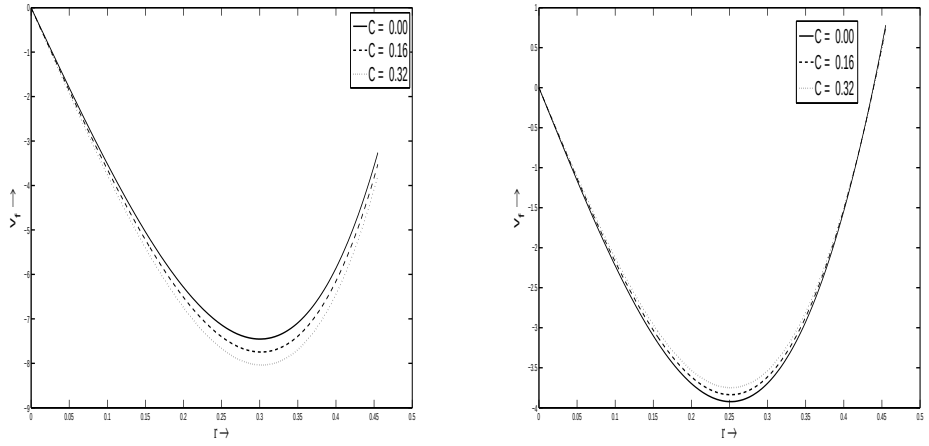

(4.6a) (4.6b)

Figure 4.6: Radial velocity profile of the fluid along the radial distance for different volume fraction of particles at $x = 0.2$ for $t = 0.3$, $\omega = 0.02$, $\phi = 0.6$, $Re_0 = 5$, $\delta = 0.08$, $\bar{Q} = 1.5$, $\bar{Q}^{(1)} = 20$, $\bar{Q}^{(2)} = 20$, $M = 1139$. Solid line, dashed line and dashed dotted line correspond respectively to $C = 0.0$, $C = 0.16$ and $C = 0.32$.

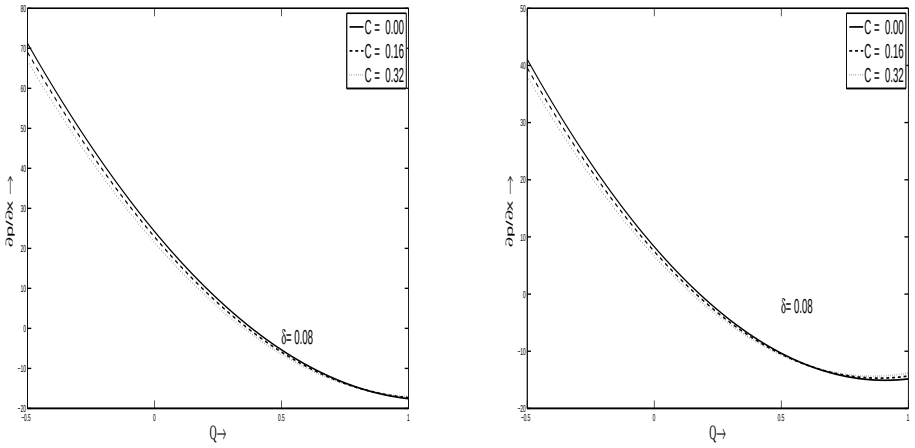

(4.7a) $\delta = 0.08$ (4.7b) $\delta = 0.08$

Figure 4.7: The effect of δ on the relation between the pressure gradient and the time-averaged volume flow rate for different volume fraction of particles with $\omega = 0.02$, $\phi = 0.6$, $Re_0 = 5$, $\bar{Q}^{(1)} = 15$, $\bar{Q}^{(2)} = 15$, $M = 1139$, $x = 0.8$, $t = 0.4$, (4.7*a*) $\delta = 0.08$, (4.7*b*) $\delta = 0.08$.

the flow while a negative one enhances it. There are several diseases like achalasia, oesophageal stricture and oesophageal tumors creating difficulty in swallowing. Pressure gradient profile suggests that patients suffering from these diseases may be advised to consume food items with less particulate suspensions. Larger pressure gradient for low volume fraction is advised for comfortable swallowing. The two plots reveal the quantitative difference between the results obtained by the present analysis Figure (4.7a) and by Pandey and Singh (2018) Figures ((4.7b).

The fluid motion is also shown by streamlines which are invisible curves in the flow field of the fluid such that the tangent at each of the points of the curve gives the direction of the local velocity at that point at an instant. Streamlines in the fixed frame with $\omega = 0.02$, $\phi = 0.6$, $Re_0 = 5$, $Re_0 = 5$, $\delta = 0.08$, $\bar{Q}^{(1)} = 20$, $\bar{Q}^{(2)} = 20$, $M = 1139$, $t = 1.0$ at different time-averaged volume flow rates

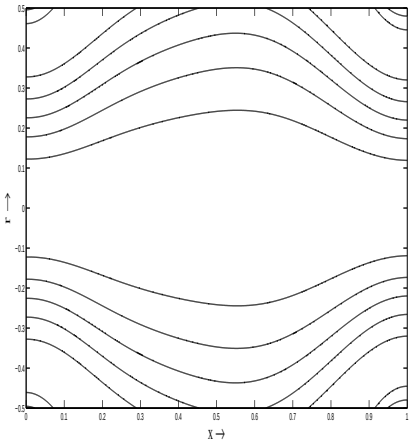

(4.8a) $\bar{Q} = 1.2$

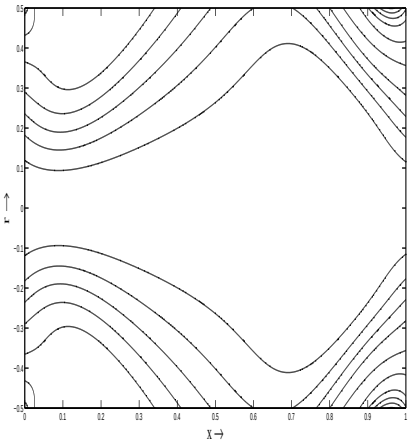

(4.8b) $\bar{Q} = 3.2$

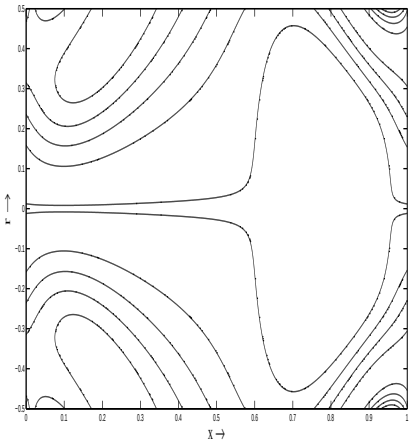

(4.8c) $\bar{Q} = 5.0$

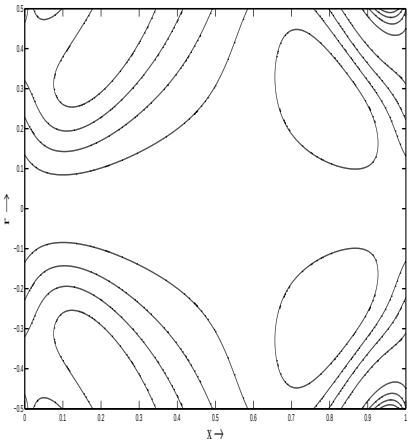

(4.8d) $\bar{Q} = 5.1$

Figure 4.8: Streamlines in the fixed frame with $\omega = 0.02$, $C = 0.12$, $\phi = 0.6$, $Re_0 = 5$, $\delta = 0.08$, $\bar{Q}^{(1)} = 20$, $\bar{Q}^{(2)} = 20$, $M = 1139$, $t = 1.0$ at different time-averaged volume flow rates (4.8a) $\bar{Q} = 1.2$, (4.8b) $\bar{Q} = 3.2$, (4.8c) $\bar{Q} = 5.0$ and (4.8d) $\bar{Q} = 5.1$.

($\bar{Q}$ = 1.2, 3.2, 5.0, 5.1) are shown in Figure 4.8. When $\bar{Q}$ is increased, the streamlines change shapes and above a certain $\bar{Q}$, the central streamline splits to surround a ring-shaped bolus of the fluid as a closed streamline as depicted in Figures (4.8b)-(4.8d). This trapped bolus is now pushed ahead along with the peristaltic wave. This leads us to infer that trapping takes place at high flow rates. Trapping was first discovered by Shapiro *et al.* (1969).

4.5 Conclusions

Peristaltic transport of particle-fluid suspension through oesophagus has been investigated theoretically by regular perturbation technique up to the second order of the wave number. The impact of volume fraction of particles on the pressure gradient and the velocity is examined and streamline patterns are obtained. The presence of particulate matter affects the pumping performance and velocity.

In the discussion section, the quantitative differences in the results obtained by us and those of Pandey and Singh (2018) who presented the results up to the first order of wave number, were compared and significant differences were observed.

It is observed that the axial velocity of the fluid exceeds that of the solid particles almost everywhere. However, at the wall the axial velocity of the fluid is zero due to the imposition of no-slip condition; but the suspended particulate material has non-zero positive axial velocity close to the wall. Thus, the axial velocity of the suspended particles near the tube wall exceeds the fluid velocity. It is also observed that the axial velocity is retrograde in the regions close to maximum occlusions paving way to instantaneous backward flow. Backward flow is

created in a small region with maximum occlusion. Hence, the net flow is positive. Further, the magnitude of the velocity at the second occlusion point is more than at the first occlusion point due to dilating wave amplitude.

A higher concentrations of suspended particulate matter diminishes the pressure gradient and hence also the axial and radial velocities. The investigation endorses the advice of the doctors to the patients suffering from achalasia, oesophageal stricture and oesophageal tumors to consume liquid or food items with lesser solid contents.

Streamline patterns are changed by increasing flow rate while trapping occurs at high flow rates.

****